JACS
JOURNAL OF THE AMERICAN CHEMICAL SOCIETY

Article

pubs.acs.org/JACS

Are There Really Low-Barrier Hydrogen Bonds in Proteins? The Case of Photoactive Yellow Protein

Marc Nadal-Ferret,[†] Ricard Gelabert,*[,†] Miquel Moreno,[†] and José M. Lluch[†,‡]

[†]Departament de Química and [‡]Institut de Biotecnologia i de Biomedicina, Universitat Autònoma de Barcelona, 08193 Bellaterra (Barcelona), Spain

Supporting Information

ABSTRACT: For a long time, low-barrier hydrogen bonds (LBHBs) have been proposed to exist in many enzymes and to play an important role in their catalytic function, but the proof of their existence has been elusive. The transient formation of an LBHB in a protein system has been detected for the first time using neutron diffraction techniques on a photoactive yellow protein (PYP) crystal in a study published in 2009 (Yamaguchi, S.; et al. *Proc. Natl. Acad. Sci. U.S.A.* **2009**, *106*, 440−444). However, very recent theoretical studies based on electronic structure calculations and NMR resonance experiments on PYP in solution (Saito, K.; et al. *Proc. Natl. Acad. Sci. U.S.A.* **2012**, *109*, 167−172) strongly indicate that there is not such an LBHB. By means of electronic structure calculations combined with the solution of the nuclear Schrödinger equation, we analyze here under which conditions an LBHB can exist in PYP, thus leading to a more reasonable and conciliating understanding of the above-mentioned studies.

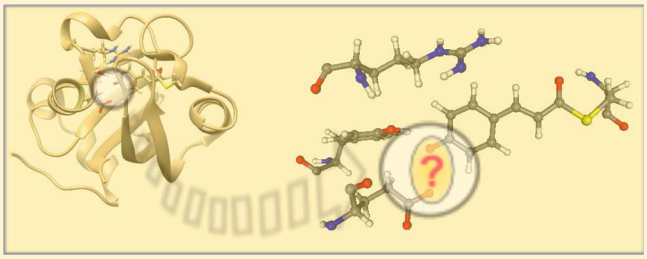

INTRODUCTION

It is widely accepted that hydrogen bonds can stabilize intermediates and transition states in enzyme reactions, in this way significantly contributing to the huge catalytic power of enzymes.[1−3] In particular, a special class of hydrogen bonds, the so-called low-barrier hydrogen bonds (LBHBs), were proposed to play an important role in enzyme catalysis around 20 years ago.[4−12] This idea provoked a flurry of activity and stimulated an intense research effort that led to opposing viewpoints about the real existence of LBHBs and their chemical properties and functions in enzyme catalysis.[13−25]

Two of the most used physicochemical parameters to try to identify an LBHB are a short distance between the hydrogen bond donor and acceptor electronegative atoms (<2.55 Å for O−H−O and <2.65 Å for O−H−N) and a far-downfield proton ^{1}H NMR chemical shift (17−19 ppm). These values turn out to be indicative, although not conclusive, of the existence of an LBHB.[2,3,20]

On the other hand, the most definitive physical characterization of an LBHB comes from its definition in terms of quantum mechanics. The potential energy hypersurface associated with a hydrogen bond can be a multidimensional double well: the two minimum energy structures, each one corresponding to the proton attached to one or the other of the electronegative atoms, are separated by a classical (i.e., without zero-point energy, ZPE) potential energy barrier. In an LBHB the classical energy barrier is low enough so that the nuclear wave function corresponding to the ground vibrational level of the double well reaches its maximum values at the region of that energy barrier. Thus, the proton can freely move in the region between the two electronegative atoms, and its bonding to them becomes essentially covalent.[5,20,23] If a monodimensional representation of the reaction path corresponding to the proton shifting is adopted, that nuclear wave function condition is fulfilled provided that the ground vibrational level of the monodimensional double well lies at or above the classical energy barrier, according to the definition given by Cleland and Kreevoy.[7] Taking all that into account, the most conclusive, direct way to identify an LBHB is the determination of the proton location by neutron diffraction measurements: if the proton is found to be in the central region between the two electronegative atoms, the hydrogen bond is an LBHB.

For the discussion ahead, it is worth mentioning that many of the reported systems containing an LBHB were simple molecules studied in the gas phase or in the crystal. Systems studied in solution had properties more akin to a structure with the proton localized near the donor atom.[26,27] According to Perrin,[27] this could be understood taking into account that even two completely symmetrical potential energy minima for the process in the gas phase would be solvated differently due to different instantaneous configurations of the solvent with the system.

Recently, Yamaguchi et al.[28] have provided the first direct demonstration of the formation of an LBHB in a protein, the photoactive yellow protein (PYP). PYP is a blue light receptor from the halophilic photosynthetic bacterium *Halorhodospira halophila*, which controls the negative phototactic response of

Received: November 15, 2013
Published: February 19, 2014

   dx.doi.org/10.1021/ja4116617 | *J. Am. Chem. Soc.* 2014, 136, 3542−3552

this organism.[29] This protein was known to contain two short hydrogen bonds adjacent to the reaction center:[30,31] one formed between the phenolic oxygen of the chromophore of PYP, *p*-coumaric acid (*p*CA), and the carboxylic oxygen of Glu46 (with a distance O···O of 2.58 Å) and the other between the phenolic oxygen of *p*CA and the phenolic oxygen of Tyr42 (with a distance O···O of 2.51 Å). Taking into account the O···O distance, both hydrogen bonds could be considered as possible LBHBs, although the hydrogen atoms involved in them had never been observed.[30−32] However, Yamaguchi et al.[28] prepared crystals with crystallization buffers made with 99.9% heavy water and identified 87% of the H/D positions in PYP by performing high-resolution (1.5 Å) neutron crystallographic analysis combined with high-resolution (1.25 Å) X-ray crystallography at room temperature. Their main results are summarized in Table 1 (see Figure 1).

Table 1. Main Measured Interatomic Distances (Å) Corresponding to the *p*CA···Glu46 and *p*CA···Tyr42 Hydrogen Bonds (HBs) in PYP

*p*CA···Glu46 HB		*p*CA···Tyr42 HB	
O(*p*CA)···O(Glu46)	2.56	O(*p*CA)···O(Tyr42)	2.52
O(*p*CA)···D	1.37	O(*p*CA)···D	1.65
O(Glu46)···D	1.21	O(Tyr42)···D	0.96

The average distance O−H (D) over all the measured hydrogen bonds was 0.95 Å. It is clear that the deuterium nucleus appears to be delocalized in the central region of the *p*CA···Glu46 hydrogen bond, being shared by the two oxygen atoms. This fact does not occur in the *p*CA···Tyr42 hydrogen bond, where the deuterium atom is covalently attached to the phenolic oxygen of Tyr42. Then, according to the measurements of Yamaguchi et al.,[28] *p*CA···Glu46 is actually an LBHB, but *p*CA···Tyr42 is not. Another important counterintuitive finding was that Arg52, a residue at a distance of 6.34 Å from the phenolic oxygen of *p*CA, is deprotonated (neutral) in the crystal, in this way being unable to stabilize the negative charge in the vicinity of the chromophore and so contributing to the formation of the LBHB.

However, in several very recent papers, Saito and Ishikita[33−35] have claimed that Arg52 should be protonated on the PYP protein surface and that the chemical properties of the *p*CA···Glu46 bond can be simply explained as a conventional hydrogen bond, without invoking the LBHB concept. In particular,[33] they have carried out quantum mechanical/molecular mechanical (QM/MM) calculations to reproduce the two short hydrogen bond distances of the crystal structure, obtaining 2.57 and 2.50 Å for *p*CA···Glu46 and *p*CA···Tyr42, respectively, but they have not found any minimum energy structure with the proton near the central region of the hydrogen bonds. In both cases, the electronic structure calculations lead to energy minima with the two protons clearly belonging to the Glu46 or Tyr42 moieties, respectively. In addition, they argue that the experimental ^{1}H NMR chemical shift (15.2 ppm) in solution[36] was assigned to protonated Glu46, which is a value smaller than that for typical LBHBs. Moreover, QM/MM calculations by Saito and Ishikita[34] suggest that the experimental chemical shift for the *p*CA···Glu46 hydrogen bond should correspond to a geometry with the proton attached to the Glu46 moiety.

At this point the controversy is raised, and it is no longer clear whether an LBHB has already been definitively determined in a protein (in the PYP in particular). In this paper we describe a theoretical study of the two short hydrogen bonds found in the photoactive yellow protein aimed at discussing the existence of such an LBHB and the source of the discrepancy among the different experimental and theoretical results available so far. As mentioned before, the fingerprint of an LBHB is the delocalization of the proton in the central region of the hydrogen bond, and this property is not determined just by the potential energy surface, but also by the nuclear probability density function of the system. Then, here, after having done the required electronic structure calculations, we have solved the suitable nuclear Schrödinger equations to obtain the nuclear wave functions and the properties of the two controversial hydrogen bonds derived from them.

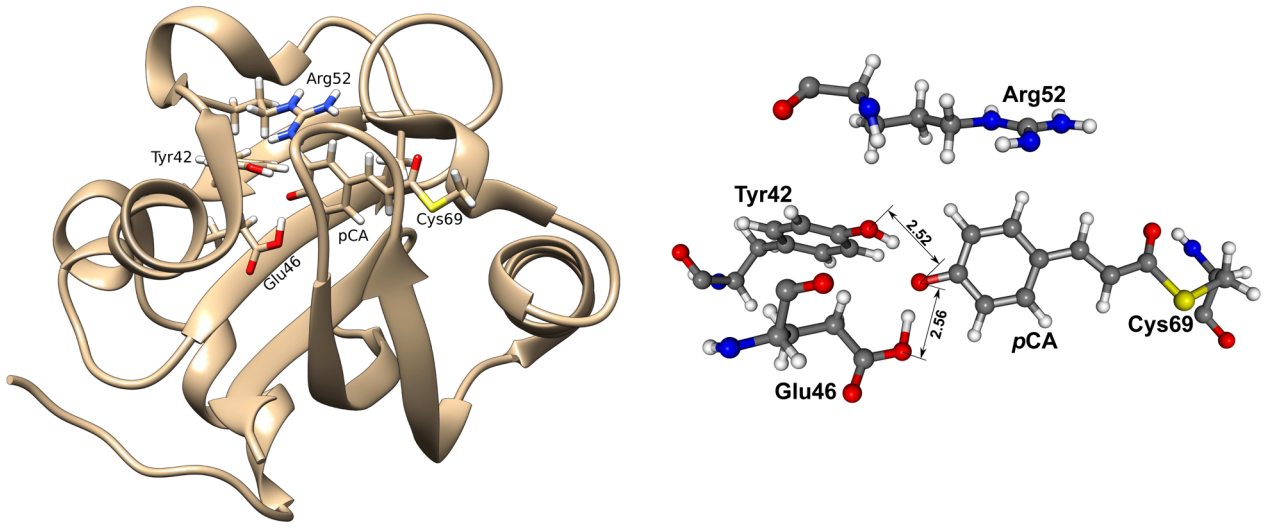

Figure 1. Structure of crystallized PYP as determined by neutron diffraction (PDB ID 2ZOI). Left: representation of PYP detailing the chromophore and surrounding residues. Right: detailed view of *p*CA and surrounding residues with distances to the closest proton acceptors (Å). Note that Arg52 is deprotonated.

dx.doi.org/10.1021/ja4116617 | *J. Am. Chem. Soc.* 2014, 136, 3542−3552

COMPUTATIONAL DETAILS

Initial Coordinates for Crystalline PYP. The starting point was the neutron diffraction structure determined by Yamaguchi et al.[28] (PDB ID 2ZOI), which contains about 87% H and D atoms. Wherever an atom appeared in two positions with different occupation numbers, the one with the highest value was selected. Missing atoms were introduced at pD 9 (the conditions of crystallization of the structure) using the PROPKA server.[37−40]

Crystalline PYP QM/MM Electronic Structure Calculations. Born−Oppenheimer potential energy was computed within a QM/MM scheme, where the chemically most relevant region of the protein is treated quantum-mechanically, while the rest of the residues and environment are described as a set of point charges according to a molecular mechanics force field. The effect of the MM part on the QM portion of the system is included by means of the so-called electronic embedding (EE), which allows the point charges of the environment to polarize the QM part, modifying its orbital description. No polarization of the MM part is taken into account. In this study, the QM region included the residues *p*CA, Glu46, Tyr42, Arg52, Thr50, and Ile31. To reproduce as closely as possible the structure reported by neutron diffraction, Arg52 was included in its neutral form.

The QM energy was calculated using the Gaussian 09[41] software, with density functional theory (DFT)[42] using the CAM-B3LYP functional[43] and the split-valence quality 6-31+G(d,p) basis set. The point charge values for the MM part of the system were obtained from the CHARMM22 force field.[44,45] Assembly of the QM and MM regions was done through the use of link atoms. Neutron diffraction data were obtained at room temperature,[28] so looking for a minimum (a structure appropriate to describe the structure at best at 0 K) is a debatable strategy. For this reason, no optimizations were considered to describe the crystalline form of PYP. Potential energy surfaces and profiles were obtained as follows: We computed a series of structures obtained by taking the structure of the protein as described before and displacing the position of the proton according to the scanned coordinate(s) and without geometry relaxation (unrelaxed potential energy scans).

When necessary, NMR isotropic shieldings were obtained through use of the gauge-invariant atomic orbital (GIAO) method for each concerned structure. Chemical shifts have been determined as the difference of isotropic shieldings of tetramethylsilane (TMS) protons and that of the concerned proton. A cautionary note needs to be issued here concerning the accuracy of chemical shifts computed in this way. In a recent review on computation of ^{1}H and ^{13}C NMR chemical shifts with theoretical methods, Lodewyk et al. reported average deviations of 0.4 ppm for the ^{1}H chemical shift (see ref 46 and references therein). It is possible to improve these computed values by means of different strategies, such as empirical scaling, which uses correlations between experimental chemical shifts and computed isotropic shieldings for a set of data molecules. While approaches like this might prove necessary to achieve experimental precision, we have not used them, as we are interested in the approximate values of ^{1}H chemical shifts for our models and the trends they display. In this case, the average error of 0.4 ppm does not compromise the interpretation of the results.

QM/MM Molecular Dynamics Simulations of PYP in Solution. The starting point was the same as detailed above for crystalline PYP, but in this case we deemed it convenient to protonate Arg52 given its pK_a and the availability of protons in solution. A water sphere of 35 Å was used to solvate the protein, placing its center at the center of mass of the protein. Once the protein was solvated, the geometry was optimized with the ChemShell software[47] using a QM/MM scheme.[48] The quantum mechanical region (which includes the residues *p*CA, Glu46, Tyr42, Arg52, Thr50, and Ile31 and three crystallographic water molecules that interact with them, 88 atoms in total) was treated with Gaussian09,[41] using DFT theory[42] with the B3LYP functional[49] and the 6-31+G(d,p) basis set. The MM region (18270 atoms) was treated by means of the CHARMM22 force field,[44,45] and the QM and MM regions are connected by link atoms. The QM/MM interaction energy was calculated with ChemShell[47] with the charge-shift scheme. That is to say, QM/MM electrostatic interactions are handled by the QM code with QM polarization due to the presence of MM charges, charges close to the link atoms are shifted away, and point dipoles are added to compensate. The optimization was done by HDLCopt[50]—another ChemShell device—with an active region including all residues with atoms within 19 Å of the chromophore.

Starting off the optimized structure, a molecular dynamics simulation had to be computed. Because LBHB interactions are absent from all force fields known to us, a QM/MM molecular dynamics simulation had to be performed. To this end, the ChemShell package DL-POLY[51] was used. The QM region included the same residues as the optimization, while the MM region included the rest of the protein and solvent molecules. The active region consisted of all the residues containing at least one atom within 15 Å of any *p*CA atom. Because the computational costs are extremely onerous with respect to MM molecular dynamics, a semiempirical Hamiltonian has been selected to deal with the QM part of the system. In particular, the QM energy was calculated with the AM1 semiempirical method[52] using the MNDO99 program,[53] and the MM was described with the CHARMM22 force field. The regions were assembled by link atoms, and the QM/MM coupling was done by means of the *shift* option in ChemShell. Even in these conditions, the simulation is very costly and only relatively short simulation times are affordable, even though the simulation suffices to assess the dynamical stability of the structure. The system was heated to 300 K in steps of 10 K. After that, the system was equilibrated for 10 ps. Finally, a 100 ps dynamics simulation was run (in 1 fs time steps) in the NVT ensemble. The parameters of this QM/MM molecular dynamics simulation are in line with current applications of this technique.

Individual snapshots were selected, and for each of them a 1-dimensional potential energy profile for the proton-transfer reaction between *p*CA and Glu46 was computed by shifting the position of the proton from donor to acceptor atoms. To perform these energy calculations, a procedure similar to that for the crystal PYP profiles was followed. That is to say, the DFT CAM-B3LYP functional with 6-31+G(d,p) was used for the QM region, which was polarized by the atoms in the MM region, treated as point charges according to the CHARMM22 force field. The chemical shift was also computed along these profiles and used (see the next section) to compute average chemical shifts.

The two functionals used in this work, B3LYP and CAM-B3LYP, differ only in the exchange-correlation part of the functional. CAM-B3LYP was developed especially for studies of excited states, where it avoids the problems that hybrid functionals have in reproducing excitation energies for charge-transfer excited states. For ground states, CAM-B3LYP has been reported to perform better than B3LYP when computing classical potential energy barriers and NMR shielding constants.[54] More recent studies have confirmed a similar performance of both functionals for ground-state proton-transfer reaction barriers.[55] See the Supporting Information for an assessment of the performance of the electronic structure method used in this work.

Anharmonic Vibrational Calculations. To determine the vibrational energy levels, the nuclear Schrödinger equation must be solved:

$$[\hat{T} + U(\mathbf{R})]\Psi(\mathbf{R}) = E\Psi(\mathbf{R}) \quad (1)$$

This is a conventional time-independent Schrödinger equation where the potential energy operator U is the potential energy surface for the motion of the proton. The potential energy surfaces in this work are either 1- or 2-dimensional, depending on the independent directions in which the shared proton is allowed to move. For 1-dimensional profiles, a total of 10 distinct geometries, obtained by shifting the position of the H from donor to acceptor, were computed, while for 2-dimensional surfaces, a total of 10 points in the x_1 and 6 points in the x_2 directions were computed, for a total of 60 points (see Figure 2 for a description of the coordinates). The resulting profiles or potential energy surfaces were fitted into cubic spline functional forms.[56] In all cases care was exercised to ensure that the border of the potential energy profiles or surfaces was "closed", that is, that all values on the

dx.doi.org/10.1021/ja4116617 | J. Am. Chem. Soc. 2014, 136, 3542−3552

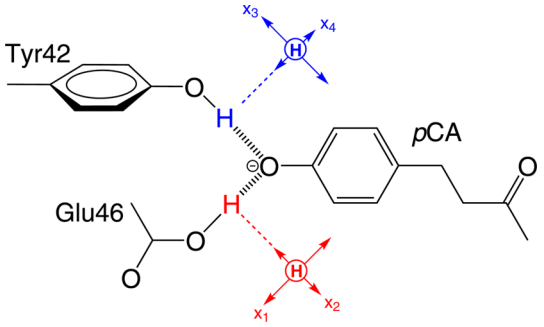

Figure 2. Description of the dynamical coordinate systems used to compute vibrational eigenstates and expected geometries of the hydrogen bonds. Coordinates for the Glu46−*p*CA hydrogen bond (x_1, x_2) are shown in red, and those for the Tyr42−*p*CA hydrogen bond (x_3, x_4) are shown in blue. The values for coordinates x_1 and x_3, which denote the main component of the position of the proton in the respective hydrogen bond, increase in going away from *p*CA.

border of the potential energy profiles or surfaces were sufficiently high with respect to the value of the energy in the minimum. This is relevant to avoid unphysical reflection effects on the vibrational wave functions computed.

To solve the nuclear Schrödinger equation, the generic discrete variable representation (DVR) proposed by Colbert and Miller was used.[57] For 1-dimensional profiles the DVR representation was taken to be 50 evenly spaced points spanning the domain of calculated geometries, whereas for 2-dimensional surfaces a regular grid of 25 × 25 points spanning the domain of x_1 and x_2 (and of x_3 and x_4) was used. After the DVR matrix representation of the Hamiltonian was constructed, its diagonalization yielded the eigenvalues $\{E\}$ (vibrational energy levels) and eigenvectors $\{\Psi\}$ (vibrational wave functions). The determined energy levels and wave functions were tested for convergence by checking for stability upon enlargement of the DVR grid. The wave functions obtained in this way were used to compute expected positions and average per-level values of the chemical shift. When computing chemical shifts, their value was calculated also on the same structures and the resulting mesh fitted for ease of computation to a cubic spline functional form. Then the level-specific values of the chemical shift are given as the weighted average of the chemical shift over all structures using as weights the values of $|\psi|^2$.

RESULTS AND DISCUSSION

From the exposition of facts laid out in the Introduction, it should be obvious that the protonation state of Arg52 is key to justifying the existence or not of an LBHB in the *p*CA···Glu46 hydrogen bond. Although it strikes up as odd that this residue be deprotonated in the experimental conditions of pD 9, it is nonetheless true that this statement comes from a *direct* determination of the positions of protons and deuterons via neutron diffraction. In the understanding that all experiments can contain mistakes or their conclusions can be based on biased interpretations, we think that the possibility of an LBHB in the crystal form of PYP needs to be reexamined using sound theoretical methods that go beyond simple topographical studies of the potential energy surface (PES).

It is our purpose to show that the disparity of apparently contradictory data described above, supporting or refuting the existence of an LBHB in PYP, can be satisfactorily explained in its entirety provided that the following is borne in mind: that PYP's structure is significantly different in crystal form and in solution at room temperature.

Crystallized PYP. The neutron diffraction experiment of Yamaguchi et al. pinpointed in an unambiguous way the position of deuterium in *p*CA···Glu46 very close to the midpoint of the hydrogen bond and that Arg52 was deprotonated. Despite the controversy on these subjects, we find that neutron diffraction experiments provide direct determination of the position of the proton/deuteron and as such hoard a value of solid evidence, and the conclusions derived from them need to be assessed more thoroughly before being written down as erroneous on the basis of theoretical calculations relying on pure topographical analyses of the potential energy surface.

In particular, some caution would be advisable with the conclusions of Saito and Ishikita on the geometry of this hydrogen bond. The geometry of a molecule should be derived in principle using the standard procedure used in quantum mechanics to determine the expected value of a certain observable. For the geometry **R** this would be

$$\langle \mathbf{R} \rangle_E = \langle E|\hat{\mathbf{R}}|E\rangle \tag{2}$$

where $|E\rangle$ denotes the eigenstate with energy E, which in this context is a vibrational state. It should be evident, then, that a varying geometry would be determined for each vibrational state.

Now, it is a well-established procedure in computational chemistry to apply the harmonic approximation to the potential energy surface at the minimum of potential energy to ease the analysis of stability, vibration, etc. This has as a consequence that the expected values of the molecular coordinates match those of the minimum of potential energy. This straightforward sequence of steps originating at the harmonic approximation for vibration is what lies implicitly behind the commonplace procedure in theoretical studies of molecular structure of (1) minimizing the Born−Oppenheimer potential energy and (2) read out of the values of the coordinates at this minimum and automatically identifying them with those that will be measured in an experiment. This is precisely the procedure followed by Saito and Ishikita to refute the existence of the LBHB between *p*CA and Glu46 in PYP (see Figure 2 in ref 33). However, even though the potential energy profiles computed by Saito and Ishikita clearly determine a minimum with H bound to Glu46, it is also clear that they contain a certain degree of anharmonicity, and thus, deviations between the actual measurements of the geometry and the expectations placed on the position of the potential energy minimum should be expected. Apparently unrelated systems such as elongated dihydrogen (and compressed dihydride) complexes are well-established examples of this phenomenon that could only be studied by theoretical methods once anharmonic vibrational analysis was considered.[58−62] A completely analogous discussion could be issued on the values of NMR-related quantities, such as chemical shifts and H−D coupling constants.[20,23,60,61]

Because of this, we firmly believe that an anharmonic vibrational analysis of the motion of the H (D) is mandatory to determine the expected position and, hence, the existence or not of an LBHB from first principles. The starting point for our study is the neutron diffraction structure (PDB ID 2ZOI) of Yamaguchi et al.[28] Consequently, we have decided to take the crystal structure as provided in the PDB as a pure experimental datum and to compute on it, exclusive of minimization, the potential energy profiles by means of QM/MM methodology, as set forth in the Computational Methods.

Let us focus on the O(*p*CA)···D···O(Glu46) hydrogen bond in crystallized PYP. A cursory analysis of this crystal structure

dx.doi.org/10.1021/ja4116617 | J. Am. Chem. Soc. 2014, 136, 3542−3552

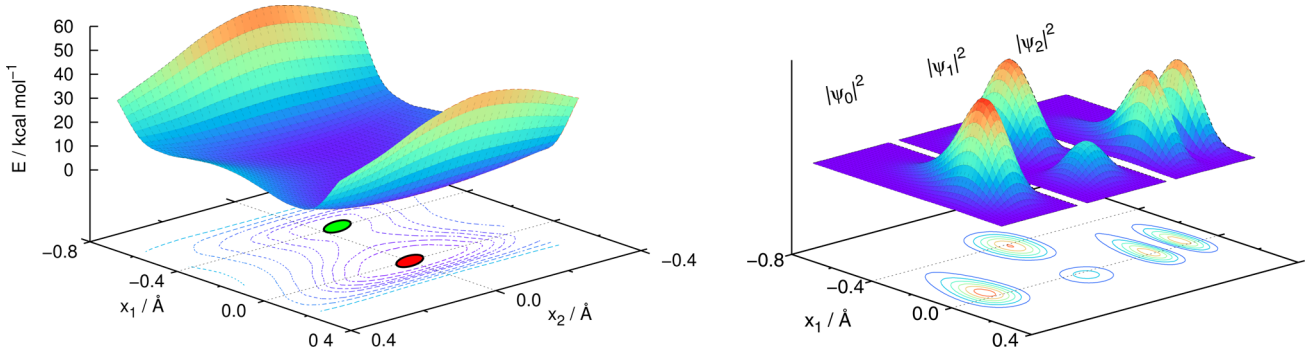

Figure 3. Results of the 2-dimensional anharmonic vibrational study of crystallized PYP. Left: potential energy surface built using the dynamical coordinates described in Figure 2. The red circle indicates the position of the absolute minimum—corresponding to the proton bound to Glu46—and the green circle that of the shallow minimum with the proton bound to *p*CA. Right: side-by-side representation of the probability density functions of the ground (ψ_0) and first excited (ψ_1) and second excited (ψ_2) vibrational states of the H-PYP system.

Table 2. Vibrational Energy Levels, Expected Values for the Distances between X = H, D and Donor and Acceptor Atoms in the *p*CA···Glu46 Hydrogen Bond, and Chemical Shifts for the 2-Dimensional Potential Energy Surface Model[a]

isotopologue	state	E (kcal mol^{-1})	d_1 (Å)	d_2 (Å)	δ (ppm)	P_{Glu46}	P_X	P_{pCA}
H-PYP	ψ_0	4.07	1.14	1.43	18.7	0.64	0.30	0.06
	ψ_1	6.61	1.34	1.22	18.2	0.22	0.17	0.61
	ψ_2	8.77	1.13	1.44	18.3	0.70	0.25	0.05
D-PYP	ψ_0	2.74	1.10	1.46	18.5	0.78	0.20	0.02
	ψ_1	4.84	1.34	1.22	19.0	0.15	0.30	0.55
	ψ_2	5.73	1.09	1.47	18.1	0.82	0.16	0.02
	ψ_3	6.61	1.27	1.29	17.9	0.31	0.30	0.39

[a]The population of chemically significant regions P_A is given for each isotopologue and for each vibrational state ψ_s, with A = Glu46 for "H (D) bound to Glu46", A = *p*CA for "H (D) bound to *p*CA", and A = X for the intermediate case. Only levels within 5 kcal mol^{-1} of the ground state are shown.

reveals that the O(*p*CA)···D···O(Glu46) hydrogen bond is not completely linear, and accordingly, we have chosen to study the motion of the H (D) on the plane defined by the positions of the three atoms involved. This has induced the definition of two orthogonal coordinates, x_1 and x_2, useful in analyzing the potential energy surface and performing the vibrational study and which are defined graphically in Figure 2. The origin for these coordinates has been conventionally assigned to the deepest minimum in the potential energy explored. For x_1 in particular, which denotes the position of H (D) along the line linking donor and acceptor atoms, positive values correspond to H (D) being closer to Glu46 and negative values to H (D) being closer to *p*CA than the minimum.

Using these coordinates, the PES has been computed and is represented in Figure 3. In agreement with the results of Saito and Ishikita, the deepest minimum is found to be in a configuration where the proton is bound to Glu46 (distances Glu46−H (D) = 1.05 Å and *p*CA−H (D) = 1.51 Å). A remarkable feature we have found is a secondary minimum 2.31 kcal mol^{-1} above the former and corresponding to H (D) being bound to *p*CA (distances Glu46−H (D) = 1.43 Å and *p*CA−H (D) = 1.13 Å). A similar minimum was also reported by Saito and Ishikita, but for a model system devoid of protein environment, that is, consisting only of Glu46 and *p*CA.[33] The existence of this secondary minimum and its energetic properties indicate a degree of anharmonicity that is likely to have severe effects on the ZPE and, as a consequence, the expected geometry of the hydrogen bond.

Pursuant to the rationale above, it is not the value of the coordinates of the minimum that should be compared to the experimental data on the geometry, but rather the expectation values of geometrical parameters derived from the anharmonic vibrational wave function. We emphasize that the 2-dimensional ZPE levels derived from the anharmonic vibrational study (see the Computational Methods) are high (4.07 kcal mol^{-1} for H-PYP, 2.74 kcal mol^{-1} for D-PYP) and are near or above the potential energy barrier for the proton transfer. This will have important effects on the "spread" of the nuclear wave functions with consequences bearing on the expected geometry. Figure 3 shows the probability densities $|\psi_s|^2$ for the first few vibrational states. Taking the ground vibrational state as an illustrative example, the probability density peaks at *slightly negative* x_1 values (which means closer to *p*CA than the minimum of potential energy would indicate) with a large "tail" toward even more negative values. As a consequence, we would anticipate the expectation value of the distance H (D)−Glu46 to be *longer* and that of H (D)−*p*CA to be *shorter* than the position of the minimum would indicate. We have computed the expectation values for x_1 and x_2 and turned them into distances to donor and acceptor atoms. The results are presented in Table 2.

The value of the D−Glu46 distance derived from the ground vibrational state is 1.10 Å, larger than that from the potential energy minimum in our reduced PES (1.05 Å) but still far from that from the neutron diffraction experiment (1.21 Å). For D−*p*CA a complementary behavior is observed (1.46 Å from vibrational analysis, 1.51 Å from the PES minimum, and 1.37 Å from neutron diffraction). The values coming from the ground vibrational state would correspond to what would be determined at 0 K, when only the ground state would be populated. Instead, experimental data were determined at 300 K. Then what should be computed is the thermal average

dx.doi.org/10.1021/ja4116617 | *J. Am. Chem. Soc.* 2014, 136, 3542−3552

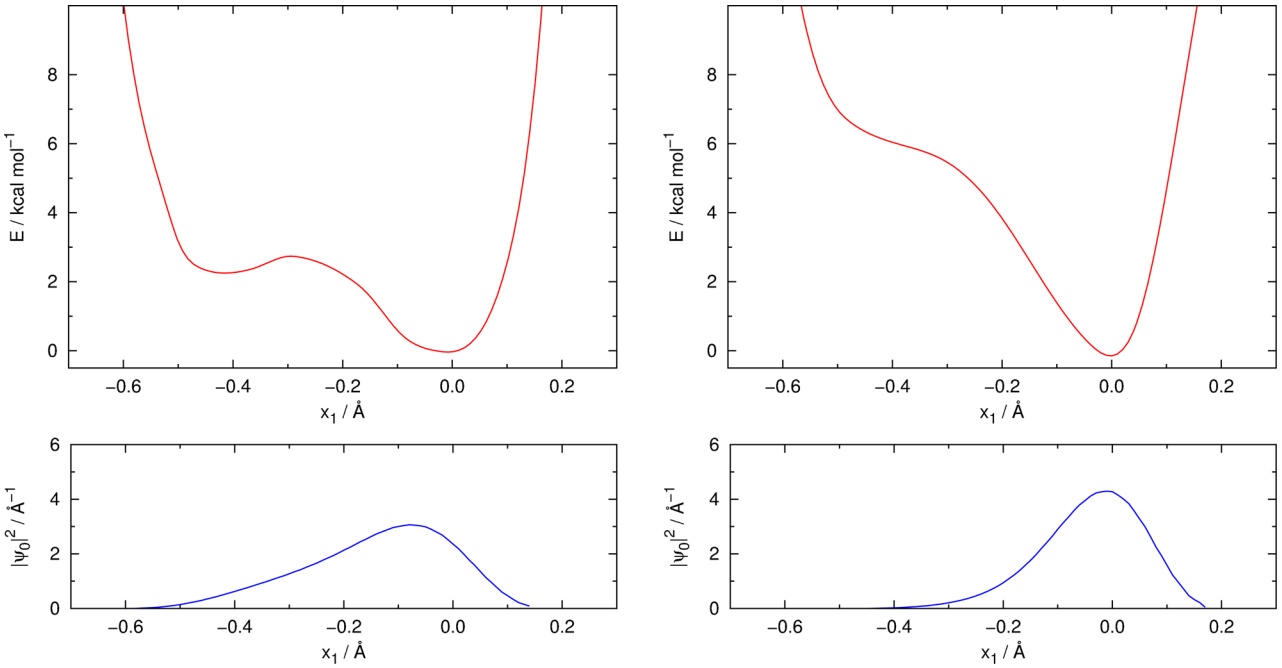

Figure 4. Top panels (in red): comparison of 1-dimensional potential energy profiles of H (D) transfer in the Glu46···*p*CA hydrogen bond for crystalline PYP when Arg52 is deprotonated (left) and protonated (right). Bottom panels (in blue): probability densities of the ground vibrational states ($|\psi_0|^2$) of H-PYP when Arg52 is deprotonated (left) and protonated (right). For the definition of x_1 see Figure 2.

(according to an equilibrium Boltzmann distribution) of the expectation values for the distances for all levels that are appreciably populated. In this, it is useful to remark that the first excited vibrational state ψ_1, being completely above the barrier, has a markedly larger expectation value for the D−Glu46 distance, which will translate into a thermal increase of the measured length and a decrease of the complementary D−*p*CA distance. Indeed, at 300 K the Boltzmann-averaged distances resulting from this consideration yield 1.11 Å for D−Glu46 and 1.45 Å for D−*p*CA. The same procedure renders the values 1.14 Å for H−Glu46 and 1.42 Å for H−*p*CA.

To obtain a quantitative measurement of the degree of delocalization of the vibrational wave functions, a different procedure has been considered, based on deriving the population of certain chemically significant regions from the wave function itself, where the regions can be in this case "H (D) bound to Glu46", "H (D) bound to *p*CA", and "H (D) in between". This can be done through the following simple formula:

$$P_A^s = \int_A |\psi_s|^2 \, d\tau \tag{3}$$

where P_A^s is the probability of finding H (D) in the region A when in vibrational state s, given by $|\psi_s|^2$. The regions are defined solely on the ranges of x_1 as follows: "H (D) bound to Glu46" corresponds to $x_1 > -0.1$, "H (D) in between" to $-0.1 > x_1 > -0.3$, and "H (D) bound to *p*CA" to $-0.3 > x_1$. Table 2 also displays this information. As can be seen, already in the ground vibrational state, the D-PYP system suffers substantial delocalization as 22% of the density is found outside the region corresponding to the deuterium bound to Glu46, this increasing to 36% in the case of H-PYP. First excited states exaggerate this behavior notably (78% for H-PYP, 85% for D-PYP). The spread of the ground-state wave function outside the neighboring area to the minimum just described is responsible for the difference we have found in the expected geometry of this hydrogen bond and that denoted by the coordinates of the potential energy minimum. The same property for the first excited state sets the trend as temperature increases, which in both isotopologues is to shorten the H (D)−*p*CA distance.

Our results indicate that the reported crystal structure, taken as is, describes a substantially anharmonic vibrational profile for the H (D) in the Glu46···*p*CA hydrogen bond and that this enlarges notably the expected D−Glu46 distance by about 0.16 Å with respect to the average O···H (D) distance over all hydrogen bonds determined in the neutron diffraction resolved structure. This enlargement reaches 0.19 Å for the expected H−Glu46 distance.

While it is not enough for a quantitative agreement with experiment, the trend shown is in the right direction and is not negligible. It must be borne in mind that effects such as crystal packing are absent from the model used and also that just one structure (in the sense of the position of the heavy atoms) is considered: because experimental data come from diffraction of a crystal at room temperature, it would be necessary to include a sample of the configurations of the protein in the crystal as befits the thermal distribution at room temperature, which would make this study unattainable. Finally, it is known that even small imprecisions in the energies of the two minima along a double-well potential have noticeable effects on the degree of (de)localization of the corresponding vibrational wave functions,[63] which will manifest themselves when computing expectation values. Thus, small errors attributable to the electronic structure methodology used contribute to the explanation of the discrepancies between experimentally measured distances and the values derived from the vibrational analysis.

Another parameter that is often invoked to discriminate the LBHB nature of a bond is the chemical shift. Saito and Ishikita computed the value of the isotropic shielding at the structure of the minimum of the PES and derived a value of 14.6 ppm.[34] Using the same rationale as above for expectation values of the

dx.doi.org/10.1021/ja4116617 | J. Am. Chem. Soc. 2014, 136, 3542−3552

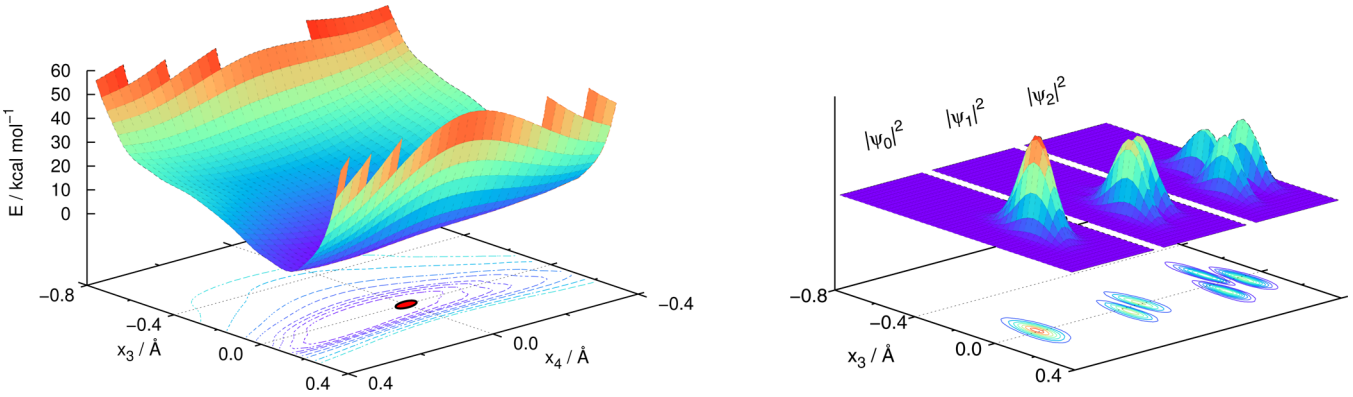

Figure 5. Results of the 2-dimensional anharmonic vibrational study of the Tyr42−*p*CA hydrogen bond. Left: potential energy surface using the dynamical coordinates described in Figure 2. The red circle denotes the position of the absolute minimum, with the proton bound to Tyr42. Right: side-by-side representation of the probability density functions of the ground (ψ_0) and first excited (ψ_1) and second excited (ψ_2) vibrational states of the H-PYP system.

Table 3. Vibrational Energy Levels, Expected Values for the Distances between X = H, D and Donor and Acceptor Atoms in the *p*CA···Tyr42 Hydrogen Bond, and Chemical Shifts for the 2-Dimensional Potential Energy Surface Model[a]

isotopologue	state	E (kcal mol^{-1})	d_1 (Å)	d_2 (Å)	δ (ppm)	P_{Tyr42}	P_X	P_{pCA}
H-PYP	ψ_0	3.68	1.03	1.50	14.0	0.85	0.15	0.00
	ψ_1	6.66	1.01	1.52	13.4	0.88	0.12	0.00
D-PYP	ψ_0	2.16	1.02	1.51	13.8	0.90	0.10	0.00
	ψ_1	4.23	1.01	1.52	13.3	0.92	0.08	0.00
	ψ_2	6.23	1.00	1.53	13.1	0.90	0.10	0.00

[a]The population of chemically significant regions P_A is given for each isotopologue and for each vibrational state ψ_s, with A = Tyr42 for "H (D) bound to Tyr42", A = *p*CA for "H (D) bound to *p*CA", and A = X for the intermediate case. Only levels within 5 kcal mol^{-1} of the ground state are shown.

geometrical parameters, the deuterium atom can be found in a plethora of different arrangements with respect to the donor and acceptor atoms, governed by the vibrational wave function. A more adequate form of computing an estimate of the chemical shift of this atom is to average the value of the chemical shift obtained at each of these arrangements using $|\psi_s|^2$ as weight, to produce vibrational level specific values of chemical shift, and then do a Boltzmann average to determine the expected value to be measured. This procedure has been applied before satisfactorily.[20,23,61,62] The values of the chemical shift for the first few vibrational levels are also presented in Table 2. The values for the ground state—adequate for very low temperature experiments—are 18.7 ppm for H-PYP and 18.5 ppm for D-PYP. These values fall well within the range commonly accepted to indicate the existence of an LBHB. This is true even for the position of the minimum in our PES (17.6 ppm).

Considering all the above, the ZPE level in the case of D-PYP lies close to the barrier of potential energy, and the wave function of this first vibrational state is spread over the full range of D coordinates. This is indicative that, in the crystal form, this hydrogen bond qualifies as an LBHB. This statement is strengthened by the value of 18.5 ppm for the chemical shift linked to the ground vibrational state of D-PYP. The LBHB character for H-PYP would be reinforced, as the ZPE is larger and, thus, the vibrational wave function for the ground state is spread out more evenly still.

A point of controversy in the literature concerned the protonation state of Arg52, as the presence of a neutral Arg52 might be seen as instrumental in stabilizing an LBHB between Glu46 and *p*CA. It is possible to assess what the role of the protonation state of this residue is by computing a 1-dimensional potential energy profile for the transfer of H (D) from Glu46 to *p*CA in the crystal structure for the two protonation states of Arg52. The results are displayed in Figure 4. A very striking difference is seen in both profiles, namely, that the secondary shallow minimum describing the situation where H (D) is bonded to *p*CA vanishes when Arg52 is protonated. Thus, changing the protonation state of Arg52 has an effect of about 4 kcal mol^{-1} on the stabilization of this secondary minimum. In fact, solving the 1-dimensional nuclear Schrödinger equation of the vibrational Hamiltonian on both profiles shows quite clearly that, if the protein is held at the structure determined in the crystal, the nuclear wave function of the ground state is essentially localized on the right well (corresponding to Glu46−H (D)···*p*CA) when Arg is protonated. On the contrary, if Arg52 is deprotonated, the wave function is delocalized with measurable amplitude over both wells, including the central region over the barrier. Thus, a situation akin to an LBHB arises only when Arg52 is deprotonated.

Let us now turn to the second short hydrogen bond, *p*CA··· Tyr42. In the crystal structure donor and acceptor atoms are 2.52 Å apart, but the shared D is found clearly in the immediate neighborhood of Tyr42's oxygen. An analogous procedure to determine the 2-dimensional vibrational eigenstates has been carried out using the x_3 and x_4 dynamical coordinates defined in Figure 2. Using these coordinates, the potential energy surface corresponding to the motion of H (D) has been computed and is shown in Figure 5. The profile shows a deep minimum at short Tyr42−H distances, and a shoulder can be seen at short *p*CA distances that fails to become a secondary minimum, in

dx.doi.org/10.1021/ja4116617 | J. Am. Chem. Soc. 2014, 136, 3542−3552

contrast to what was found for the Glu46−*p*CA hydrogen bond. The vibrational states have been computed, and a summary of the lowest lying states and expectation values of the geometry are shown in Table 3, while plots of the probability densities can be seen in Figure 5. The contrast with the Glu46−*p*CA hydrogen bond case is striking: the wave function for the ground state is confined closer to the minimum at $(x_3, x_4) = (0, 0)$, the lowest lying excited states spread actually along x_4 (which is a sideways motion of the proton) rather than along x_3, and hence, the expected geometries within each vibrational state are very similar to each other and to that of the potential energy minimum (d_1 = 1.01 Å, d_2 = 1.51 Å). There is little doubt, in view of the above, that H (D) is to be found always bound to Tyr42. Analysis of the population of the chemically relevant areas of the Tyr42···*p*CA hydrogen bond (Table 3) reveals that there is no effective population of the "H (D) bound to *p*CA" region, while at least 85% population is to be found in the "H (D) bound to Tyr42" region. A varying, but small, portion of at most 15% of the population is in the central area. This is in sharp contrast to the Glu46−*p*CA hydrogen bond (Table 2), where the central region was populated to 30% in H-PYP. To summarize, H (D) is much more localized in this hydrogen bond. In this analysis, we have used the definition that "H (D) bound to Tyr42" corresponds to $x_3 > -0.1$, "H (D) in between" to $-0.1 > x_3 > -0.3$, and "H (D) bound to *p*CA" to $-0.3 > x_3$.

As could be expected, computation of expected chemical shifts for the vibrational ground states yields values of 14.0 ppm (H) and 13.8 ppm (D), well below the range where an LBHB can be suspected. Excited vibrational states yield values of the chemical shift even smaller, which causes predicted values of the chemical shift at temperatures higher than absolute zero to be smaller than those for the ground states.

For all practical purposes the Tyr42···*p*CA hydrogen bond is not an LBHB, but a short hydrogen bond with the H (D) clearly bound to Tyr42.

Solvated PYP. In the preceding section we have shown that the neutron diffraction structure (including a deprotonated Arg52) brings about a situation with large anhamonicities for the H (D) motion along the proton-transfer coordinate between *p*CA and Glu46. This in turn causes the ground vibrational state to lie at or above the potential energy barrier and results in the largest probability of finding H (D) lying at the center of the hydrogen bond. In this sense, it can be said that the claim of Yamaguchi et al. that keeping Arg52 neutral would make the LBHB necessary to stabilize the negative charge on *p*CA is vindicated by our solid-state results.

Our calculations for crystallized PYP also predict a very low field signal for the transferring proton, which further supports the claim that this is indeed an LBHB. Nevertheless, Sigala et al. reported that the proton shared by *p*CA and Glu46 appears with a chemical shift of 15.2 ppm in solution NMR experiments.[36] This value lies well outside the range accepted for an LBHB (17−19 ppm), and this was one of the key points raised by Saito and Ishikita[33] to refute the existence of such an LBHB. In fact, the strongest criticism raised by Saito and Ishikita to the conclusions of Yamaguchi concerns the protonation state of Arg52. The rationale of this criticism was that Arg52 has a very high pK_a value and should be protonated, which should weaken the hydrogen bond between *p*CA and Glu46, such that under these conditions it will likely not be an LBHB.

We think that the disparate results on the existence or not of an LBHB in PYP can be explained by accepting that both experiments refer to *different* systems or, rather, the same system in two different states. It is not unheard of that a given biological macromolecule shows substantial differences in structure between the crystalline state and solution.[64] The structure of PYP is such that *p*CA is not deeply buried in the structure and Arg52 is actually placed as if it were a "lid" over *p*CA and in direct contact with the solvent bulk (see Figure 1). Now, if solution (as opposed to crystal) conditions are considered, it is reasonable to expect Arg52 to be protonated, as it is in contact with the solvent bulk. This will indeed affect the energetics of the *p*CA···Glu46 hydrogen bond, weakening it from its situation when Arg52 is deprotonated and causing the chemical shift to drop out of the LBHB range. To test this end, we have taken the crystal structure and protonated the Arg52 residue as proposed by Saito and Ishikita. We have determined the average chemical shift value derived from the 1-dimensional probability density, which produces a value of 18.5 ppm for the transferring proton in the ground vibrational state and 17.9 ppm for deuterium (see Figure 4), which is only slightly smaller than the value obtained for deprotonated Arg52 and would still be thought to correspond to an LBHB (although we have already shown above that the nuclear wave function in the crystal with protonated Arg52 is localized on the Glu46−H (D)···*p*CA well). We conclude from this result that changing the protonation state of Arg52 does not seem to be the only reason for the low chemical shift of the transferring proton determined by Sigala et al.[36]

Now, if the system is studied in solution at room temperature, it will be subject to thermal jitter, which could affect the dynamical stability of the hydrogen bond network over time. It is reasonable to expect that this would cause the average donor−acceptor distance of any hydrogen bond to enlarge noticeably.

As mentioned in the Introduction, this is in line with what Perrin et al. found when studying the changes undergone by alleged gas-phase/crystal LBHB-containing systems when put in solution.[26,27]

For these reasons we think that conditions in solution differ drastically from those in the crystal state and need to be addressed in an adequate way if the trends introduced are to be assessed reliably. The proper procedure involves tracking the evolution of the system in solution along a dynamical trajectory at room temperature. The possibility that an LBHB is present in the relevant part of the system rules out the possibility of standard MM simulations as none of these have been parametrized to describe this kind of interaction, and a much costlier QM/MM trajectory has to be computed instead.

The specific details are given in the Computational Methods. A water droplet of 35 Å radius is used to reproduce the environment of the protein in solution. Figure 6 depicts the solvated system. While it is not possible to fully reproduce bulk solvent conditions in this way, this picture shows that a rather thick layer of solvent molecules surrounds the protein and that it is legitimate to assume that the main effects of the interaction with the solvent will be reproduced in this setup.

The dynamics shows that the *p*CA···Glu46 hydrogen bond is still well formed over time with a mean elongation of ∼2.9 Å (see Figure 7). This reveals a substantially stretched hydrogen bond compared to the situation in the crystal structure (2.56 Å). Even though the quantitative magnitude of the change has to be taken with care due to the approximations incurred in the

dx.doi.org/10.1021/ja4116617 | J. Am. Chem. Soc. 2014, 136, 3542−3552

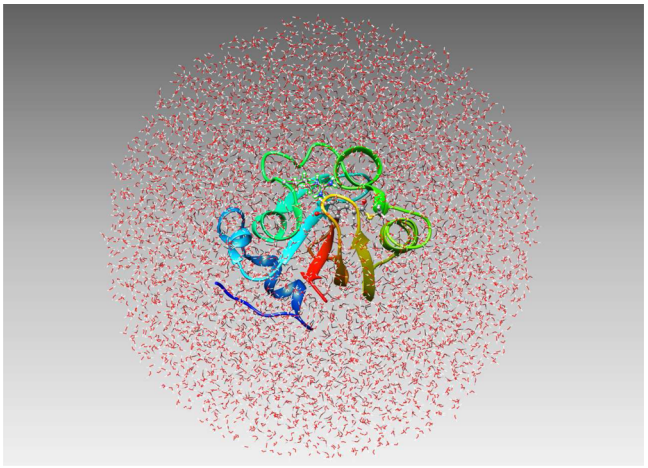

Figure 6. Depiction of the system used to study PYP in a water solution. The diameter of the water droplet is 70 Å, and a spherical concentric layer of ∼20 Å thickness surrounds the protein.

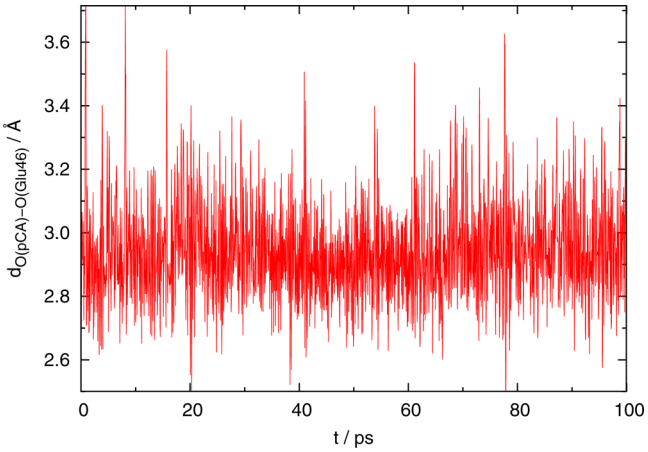

Figure 7. Time evolution of the *p*CA−Glu46 hydrogen bond distance along the QM/MM molecular dynamics simulation.

simulation, it is still very reasonable that thermal agitation increases the average O−O distance from its value in the crystalline structure.

The substantial enlargement of the *p*CA−Glu46 distance, together with Arg52 being protonated while in solution, represents a meaningful change in the energetics and dynamics of the putative LBHB. Does it still qualify as one? To answer this question, we need access to the energy landscape of the proton transfer in structures visited by the trajectory. We have picked at random some structures sampled by the trajectory that have selected *p*CA···Glu46 O−O distances. For each structure a 1-dimensional potential energy profile for the proton transfer has been computed using the same QM/MM methodology used before for the crystal structure calculations by displacing the H atom from donor to acceptor atoms, and this profile has been used to derive the vibrational eigenvalues and eigenvectors. The latter have been used to compute the expected value of the chemical shift. A few of the values computed are shown in Table 4.

The range of *p*CA···Glu46 O−O distances explored covers the shortest range explored by the QM/MM MD simulation, namely, between 2.61 and 2.76 Å (which represents about 5% of the structures). On the grounds of the chemical shift computed, we observe a very clear trend to lower chemical

Table 4. Zero-Point Energies, Expected Values of the O(Glu46)···H Distance, and Average Chemical Shift Values for Selected Structures along the QM/MM Molecular Dynamics in Solution at 300 K

$d_{O(Glu46)-pCA}$ (Å)	E (kcal mol^{-1})	$\langle d_{O(Glu46)-H}\rangle$ (Å)	$\langle\delta\rangle$ (ppm)
2.61	3.62	1.06	16.4
2.66	3.52	1.07	15.1
2.71	4.27	1.02	13.7

shifts with increasing O−O distance, indicative within current precision of a trend toward a "normal" hydrogen bond. For the majority of other structures (those with *p*CA···Glu46 O−O distances beyond 2.76 Å), it is expected that the chemical shift will remain basically constant at this value.

Summarizing, inclusion of thermal jitter *and* protonation of Arg52 in solution causes the structure of the *p*CA···Glu46 hydrogen bond to weaken and become a conventional hydrogen bond.

The general concept that LBHBs determined in the solid or gas phase vanish when the system is studied in solution is not new. Perrin et al. studied some years ago several systems that showed LBHB character in the gas phase or solid state and found that these systems existed as two tautomers in solution.[26,65−70] They explained this behavior by invoking the concept of "solvatomers",[25,27] meaning by this that the tautomers are affected by the solvent disposition, and in the understanding that even a molecule whose H-transfer could be described by a completely symmetric double well would see this symmetry lifted because of interactions with instantaneous solvent configurations.

In recent results obtained with combined low-temperature NMR/UV−vis spectroscopies on model systems related to PYP, Limbach and co-workers found that strong/short hydrogen-bonded systems would display dual bands in the UV−vis spectrum.[71] This was again, in line with Perrin's solvatomer concept,[27] interpreted as the independent existence of two tautomeric states. Interestingly, they report an estimation of the O···O distance for the analogue hydrogen bond to Glu46···*p*CA of about 2.50−2.53 Å,[72] which is shorter than the one we have found. However, in assessing this result, it is necessary to take into account that they refer to different systems, as well as the fact that our QM/MM dynamics simulation is approximate.

A more in-depth analysis of this QM/MM simulation and a comparison to the QM/MM simulation of PYP in solution with deprotonated Arg52 can be found in the Supporting Information.

CONCLUSIONS

In the preceding sections we have developed the thesis that the contradictory experimental data on the existence or not of an LBHB in the *p*CA···Glu46 hydrogen bond in PYP can be reconciled if it is accepted that the structures of PYP in solution and in the crystal state differ in some key aspects.

Taking the neutron diffraction structure at face value (which includes accepting that Arg52 is neutral), we have shown that the H (D) motion along the proton-transfer coordinate is very anharmonic. Properly considering vibrational wave functions instead of the potential energy minimum to derive expected values of the position of the H (D) atom, we have found them very close to the central region of the aforementioned hydrogen bond, giving support to the existence of an LBHB in the

dx.doi.org/10.1021/ja4116617 | J. Am. Chem. Soc. 2014, 136, 3542−3552

crystalline state. Computation of vibrationally and thermally averaged values of the chemical shift has produced a value of this magnitude in line with the range for LBHBs.

The sole experimental datum indicative of the fact that *p*CA···Glu46 is not an LBHB comes from the 15.2 ppm value of the chemical shift in solution. Because Arg52 sits between *p*CA and the bulk solvent, it is reasonable that in solution this residue is protonated. Added to this, the thermal jitter that would be present in solution at room temperature helps in determining an increased O−O distance for this hydrogen bond. In these conditions, the same procedure as in the crystal phase carried on different snapshots of a QM/MM molecular dynamics simulation has revealed that even for the shortest distances encountered in the simulation the proton is very localized next to Glu46. The computed values of the chemical shift in these circumstances are in line with those for a conventional hydrogen bond.

For all the above, our work supports the dual result that, in the solid (crystal) phase, PYP presents an LBHB in the *p*CA··· Glu46 hydrogen bond, whereas in solution this strong interaction is gone and shows characteristics of a "normal" hydrogen bond, much in line with what was found for many simpler systems by Perrin et al.[26,27] Then our results support the first direct experimental demonstration of the formation of an LBHB in a protein.

■ ASSOCIATED CONTENT

Supporting Information

Comparison of the QM/MM simulation of solvated PYP with Arg52 protonated with a QM/MM simulation of solvated PYP with neutral Arg52, assessment of the precision of the electronic structure methodology used to determine potential energy surfaces, and complete refs 41, 44, and 48. This material is available free of charge via the Internet at http://pubs.acs.org/.

■ AUTHOR INFORMATION

Corresponding Author

ricard.gelabert@uab.cat

Notes

The authors declare no competing financial interest.

■ ACKNOWLEDGMENTS

This work was supported by the Ministerio de Economía y Competitividad through Project CTQ2011-24292 and by the Generalitat de Catalunya through Project 2009SGR409. Use of the computational facilities at the Centre de Serveis Científics i Acadèmics de Catalunya (CESCA) is gratefully acknowledged. M.N.-F. thanks the Secretaria d'Universitats i Recerca (SUR) of the Departament d'Economia i Coneixement (DEC) of the Generalitat de Catalunya and the European Social Fund (ESF) for a fellowship within the FI-DGR program.

■ REFERENCES

(1) Hibbert, F.; Emsley, J. *Adv. Phys. Org. Chem.* **1991**, *26*, 255−379.
(2) Guthrie, J. P. *Chem. Biol.* **1996**, *3*, 162−170.
(3) Warshel, A.; Papazyan, A. *Proc. Natl. Acad. Sci. U.S.A.* **1996**, *93*, 13665−13670.
(4) Cleland, W. W. *Biochemistry* **1992**, *31*, 317−319.
(5) Gerlt, J. A.; Gassman, P. G. *J. Am. Chem. Soc.* **1993**, *115*, 11552−11568.
(6) Gerlt, J. A.; Gassman, P. G. *Biochemistry* **1993**, *32*, 11943−11952.
(7) Cleland, W. W.; Kreevoy, M. M. *Science* **1994**, *264*, 1887−1890.
(8) Frey, P. A.; Whitt, S. A.; Tobin, J. B. *Science* **1994**, *264*, 1927−1930.
(9) Kenyon, G. L.; Gerlt, J. A.; Petsko, G. A.; Kozarich, J. W. *Acc. Chem. Res.* **1995**, *28*, 178−186.
(10) Xiang, S. B.; Short, S. A.; Wolfenden, R.; Carter, C. W. *Biochemistry* **1995**, *34*, 4516−4523.
(11) Cleland, W. W.; Kreevoy, M. M. *Science* **1995**, *269*, 104−104.
(12) Frey, P. A. *Science* **1995**, *269*, 104−106.
(13) Warshel, A.; Papazyan, A.; Kollman, P. A. *Science* **1995**, *269*, 102−104.
(14) Schwarz, B.; Drueckhammer, D. G. *J. Am. Chem. Soc.* **1995**, *117*, 11902−11905.
(15) Alagona, G.; Ghio, C.; Kollman, P. A. *J. Am. Chem. Soc.* **1995**, *117*, 9855−9862.
(16) Scheiner, S.; Kar, T. *J. Am. Chem. Soc.* **1995**, *117*, 6970−6975.
(17) Tobin, J. B.; Whitt, S. A.; Cassidy, C. S.; Frey, P. A. *Biochemistry* **1995**, *34*, 6919−6924.
(18) Shan, S. O.; Herschlag, D. *Proc. Natl. Acad. Sci. U.S.A.* **1996**, *93*, 14474−14479.
(19) Garcia-Viloca, M.; González-Lafont, A.; Lluch, J. M. *J. Phys. Chem. A* **1997**, *101*, 3880−3886.
(20) Garcia-Viloca, M.; Gelabert, R.; González-Lafont, A.; Moreno, M.; Lluch, J. M. *J. Phys. Chem. A* **1997**, *101*, 8727−8733.
(21) Garcia-Viloca, M.; González-Lafont, A.; Lluch, J. M. *J. Am. Chem. Soc.* **1997**, *119*, 1081−1086.
(22) Perrin, C. L.; Nielson, J. B. *Annu. Rev. Phys. Chem.* **1997**, *48*, 511−544.
(23) Garcia-Viloca, M.; Gelabert, R.; González-Lafont, A.; Moreno, M.; Lluch, J. M. *J. Am. Chem. Soc.* **1998**, *120*, 10203−10209.
(24) Cleland, W. W. *Adv. Phys. Org. Chem.* **2010**, *44*, 1−17.
(25) Perrin, C. L. *Acc. Chem. Res.* **2010**, *43*, 1550−1557.
(26) Perrin, C. L. *Science* **1994**, *266*, 1665−1668.
(27) Perrin, C. L.; Lau, J. S. *J. Am. Chem. Soc.* **2006**, *128*, 11820−11824.
(28) Yamaguchi, S.; Kamikubo, H.; Kurinara, K.; Kuroki, R.; Niimura, N.; Shimizu, N.; Yamazaki, Y.; Kataoka, M. *Proc. Natl. Acad. Sci. U.S.A.* **2009**, *106*, 440−444.
(29) Sprenger, W. W.; Hoff, W. D.; Armitage, J. P.; Hellingwerf, K. J. *J. Bacteriol.* **1993**, *175*, 3096−3104.
(30) Anderson, S.; Crosson, S.; Moffat, K. *Acta Crystallogr., D* **2004**, *60*, 1008−1016.
(31) Fisher, S. Z.; Anderson, S.; Henning, R.; Moffat, K.; Langan, P.; Thiyagarajan, P.; Schultz, A. J. *Acta Crystallogr., D* **2007**, *63*, 1178−1184.
(32) Getzoff, E. D.; Gutwin, K. N.; Genick, U. K. *Nat. Struct. Biol.* **2003**, *10*, 663−668.
(33) Saito, K.; Ishikita, H. *Proc. Natl. Acad. Sci. U.S.A.* **2012**, *109*, 167−172.
(34) Saito, K.; Ishikita, H. *Biochemistry* **2012**, *51*, 1171−1177.
(35) Saito, K.; Ishikita, H. *Biochim. Biophys. Acta, Bioenerg.* **2013**, *1827*, 387−394.
(36) Sigala, P. A.; Tsuchida, M. A.; Herschlag, D. *Proc. Natl. Acad. Sci. U.S.A.* **2009**, *106*, 9232−9237.
(37) Li, H.; Robertson, A. D.; Jensen, J. H. *Proteins* **2008**, *61*, 704−721.
(38) Bas, D. C.; Rogers, D. M.; Jensen, J. H. *Proteins* **2008**, *73*, 765−783.
(39) Olsson, M. H. M.; Sondergard, C. R.; Rostkowski, M.; Jensen, J. H. *J. Chem. Theory Comput.* **2011**, *7*, 525−537.
(40) Sondergard, C. R.; Olsson, M. H. M.; Rostkowski, M.; Jensen, J. H. *J. Chem. Theory Comput.* **2011**, *7*, 2284−2295.
(41) Frisch, M. J.; et al. *Gaussian 09*, revision C.01; Gaussian Inc.: Wallingford, CT, 2009.
(42) Parr, R. G.; Yang, W. *Density Functional Theory of Atoms and Molecules*; Oxford University Press: Oxford, U.K., 1989.
(43) Yanai, T.; Dew, D. P.; Handy, N. C. *Chem. Phys. Lett.* **2004**, *393*, 51−57.
(44) MacKerell, A. D.; et al. *J. Phys. Chem. B* **1998**, *102*, 3586−3616.

(45) MacKerell, A. D.; Feig, M.; Brooks, C. L. *J. Am. Chem. Soc.* **2004**, *126*, 698−699.
(46) Lodewyk, M. W.; Siebert, M. R.; Tantillo, D. J. *Chem. Rev.* **2012**, *112*, 1839−1862.
(47) ChemShell, a Computational Chemistry Shell. www.chemshell.org (accessed Feb 4, 2014).
(48) Sherwood, P.; et al. *J. Mol. Struct.: THEOCHEM* **2003**, *632*, 1−28.
(49) Becke, A. D. *J. Chem. Phys.* **1993**, *98*, 5648−5652.
(50) Billeter, S. R.; Turner, A. J.; Thiel, W. *Phys. Chem. Chem. Phys.* **2000**, *2*, 2177−2186.
(51) Smith, W.; Forester, T. *J. Mol. Graphics* **1996**, *14*, 136−141.
(52) Dewar, M. J. S.; Zoebisch, E. G.; Healy, E. F.; Stewart, J. J. P. *J. Am. Chem. Soc.* **1985**, *107*, 3902−3909.
(53) Thiel, W. *MNDO99 Program*, version 7.0; Max-Planck-Institut für Kohlenforschung: Mülheim, Germany, 2005.
(54) Peach, M. J. G.; Helgaker, T.; Sałek, P.; Keal, T. W.; Lutnæs, O. B.; Tozer, D. J.; Handy, N. C. *Phys. Chem. Chem. Phys.* **2006**, *8*, 558−562.
(55) Wang, Y.-G. *J. Phys. Chem. A* **2009**, *113*, 10873−10879.
(56) Press, W. H.; Flannery, B. P.; Teukolsky, S. A.; Vetterling, W. T. *Numerical Recipes in Fortran*, 2nd ed.; Cambridge University Press: Cambridge, U.K., 1992.
(57) Colbert, D. T.; Miller, W. H. *J. Chem. Phys.* **1992**, *96*, 1982−1991.
(58) Gelabert, R.; Moreno, M.; Lluch, J. M.; Lledós, A. *J. Am. Chem. Soc.* **1997**, *119*, 9840−9847.
(59) Gelabert, R.; Moreno, M.; Lluch, J. M.; Lledós, A. *J. Am. Chem. Soc.* **1998**, *120*, 8168−8176.
(60) Gelabert, R.; Moreno, M.; Lluch, J. M.; Lledós, A.; Pons, V.; Heinekey, D. M. *J. Am. Chem. Soc.* **2004**, *126*, 8813−8822.
(61) Gelabert, R.; Moreno, M.; Lluch, J. M.; Lledós, A.; Heinekey, D. M. *J. Am. Chem. Soc.* **2005**, *127*, 5632−5640.
(62) Gelabert, R.; Moreno, M.; Lluch, J. M. *Chem.—Eur. J.* **2005**, *11*, 6315−6325.
(63) Gelabert, R.; Moreno, M.; Lluch, J. M. *J. Comput. Chem.* **1994**, *15*, 125−131.
(64) Klinman, J. P. *Biochemistry* **2013**, *52*, 2068−2077.
(65) Perrin, C. L.; Thoburn, J. D. *J. Am. Chem. Soc.* **1989**, *111*, 8010−8012.
(66) Perrin, C. L.; Thoburn, J. D. *J. Am. Chem. Soc.* **1992**, *114*, 8559−8565.
(67) Perrin, C. L.; Nielson, J. B. *J. Am. Chem. Soc.* **1997**, *119*, 12734−12741.
(68) Perrin, C. L.; Kim, Y. J. *J. Am. Chem. Soc.* **1998**, *120*, 12641−12645.
(69) Perrin, C. L.; Ohta, B. K. *J. Am. Chem. Soc.* **2001**, *123*, 6520−6526.
(70) Perrin, C. L.; Ohta, B. K. *Bioorg. Chem.* **2002**, *30*, 3−15.
(71) Koeppe, B.; Tolstoy, P. M.; Limbach, H.-H. *J. Am. Chem. Soc.* **2011**, *133*, 7897−7908.
(72) Koeppe, B.; Guo, J.; Tolstoy, P. M.; Denisov, G. S.; Limbach, H.-H. *J. Am. Chem. Soc.* **2013**, *135*, 7553−7566.